Acta Biomaterialia 10 (2014) 5043–5054

Contents lists available at ScienceDirect

Acta Biomaterialia

journal homepage: www.elsevier.com/locate/actabiomat

Evaluation of decellularization protocols for production of tubular small intestine submucosa scaffolds for use in oesophageal tissue engineering

Omaer Syed [a], Nick J. Walters [a], Richard M. Day [b], Hae-Won Kim [c,d], Jonathan C. Knowles [a,c,*]

[a] Division of Biomaterials and Tissue Engineering, UCL Eastman Dental Institute, 256 Grays Inn Road, London WC1X 8LD, UK
[b] Applied Biomedical Engineering Group, Division of Medicine, University College London, Gower St, London WC1E 6BT, UK
[c] Department of Nanobiomedical Science & BK21 Plus NBM Global Research Center for Regenerative Medicine, Dankook University, Cheonan 330-714, Republic of Korea
[d] Institute of Tissue Regeneration Engineering & College of Dentistry, Dankook University, Cheonan 330-714, Republic of Korea

ARTICLE INFO

Article history:
Received 28 January 2014
Received in revised form 24 July 2014
Accepted 22 August 2014
Available online 27 August 2014

Keywords:
SIS
Small intestine submucosa
Triton X-100
Tubular
SDS

ABSTRACT

Small intestine submucosa (SIS) has emerged as one of a number of naturally derived extracellular matrix (ECM) biomaterials currently in clinical use. In addition to clinical applications, ECM materials form the basis for a variety of approaches within tissue engineering research. In our preliminary work it was found that SIS can be consistently and reliably made into tubular scaffolds which confer certain potential advantages. Given that decellularization protocols for SIS are applied to sheet-form SIS, it was hypothesized that a tubular-form SIS would behave differently to pre-existing protocols. In this work, tubular SIS was produced and decellularized by the conventional peracetic acid–agitation method, peracetic acid under perfusion along with two commonly used detergent–perfusion protocols. The aim of this was to produce a tubular SIS that was both adequately decellularized and possessing the mechanical properties which would make it a suitable scaffold for oesophageal tissue engineering, which was one of the goals of this work. Analysis was carried out via mechanical tensile testing, DNA quantification, scanning electron and light microscopy, and a metabolic assay, which was used to give an indication of the biocompatibility of each decellularization method. Both peracetic acid protocols were shown to be unsuitable methods with the agitation-protocol-produced SIS, which was poorly decellularized, and the perfusion protocol resulted in poor mechanical properties. Both detergent-based protocols produced well-decellularized SIS, with no adverse mechanical effects; however, one protocol emerged, SDS/Triton X-100, which proved superior in both respects. However, this SIS showed reduced metabolic activity, and this cytotoxic effect was attributed to residual reagents. Consequently, the use of SIS produced using the detergent SD as the decellularization agent was deemed to be the most suitable, although the elimination of the DNase enzyme would give further improvement.

1. Introduction

The oesophagus as an organ can be affected by a number of medical conditions which may necessitate the need for extensive treatment to correct. These conditions can be congenital, such as oesophageal atresia, which is a paediatric condition where the oesophagus forms incorrectly, or alternatively they can be acquired conditions, such as oesophageal cancer [1–3]. Treatment for these conditions can include complicated surgical procedures, such as gastric transposition or intestinal interposition [4]. These techniques are unfortunately associated with a number of post-operative complications, including stricture formation, anastomotic leakages, dysphagia, dysmotility and gastro-oesophageal reflux, which can itself can lead to abnormal cell growth, potentially leading to neoplasia [5,6]. One approach which may provide an alternative is the use of tissue engineering to creative a viable biomaterial-based replacement for oesophageal tissue.

Clinically successful extracellular matrix (ECM) materials predominantly consist of allogeneic and xenogeneic decellularized tissues. Those tissues commonly in use are urinary bladder matrix, skin, pericardium and small intestine submucosa (SIS), which have all been used for a variety of clinical applications and are derived from human, bovine and porcine sources [7]. The benefits of ECM materials, such as SIS, are related to their effects post-implantation, including the release of growth factors and biologically active cryptic peptides upon degradation, which then influence the important processes of angiogenesis, mononuclear infiltration, cell proliferation, cell migration and cellular differentiation [8,9]. The materials

* Corresponding author at: Division of Biomaterials and Tissue Engineering, UCL Eastman Dental Institute, 256 Grays Inn Road, London WC1X 8LD, UK.
E-mail address: j.knowles@ucl.ac.uk (J.C. Knowles).

http://dx.doi.org/10.1016/j.actbio.2014.08.024
1742-7061/

are considered to not promote a rejection response but instead elicit a limited immune response restricted to Th2 lymphocytes, in line with graft acceptance, and which differs from the Th1 lymphocyte-mediated response commonly associated with xenogeneic graft rejection [10,11]. There is also an increased presence of alternatively activated M2 macrophages and associated low levels of pro-inflammatory cytokines [12,13]. In summary, the advantages of SIS include relatively rapid degradation by non-immunogenic means and a restricted immune response, in conjunction with the release of growth factors which can contribute towards constructive tissue remodelling and new tissue formation [14].

SIS has successfully been used as an oesophageal patch within *in vivo* models for the repair of the oesophagus [15,16]. However, SIS sutured into a tubular form and used for segmental oesophageal replacement in a canine model did not function well, with stenosis and detachment being the major causes of failure [17]. The mechanical properties, including the stress to failure of the material, were given as one of the principle causes for this failure and it was proposed that, had a biodegradable stent been present during the initial 3 month period, when the majority of failures occurred, it may have been possible to prevent some of the observed failures. This is in accordance with the consensus view that one of the major limitations of ECM materials such as SIS is that they do not possess the mechanical properties for relatively large tissue reconstruction roles or for resisting the stresses present in applications like rotator-cuff injury repair, where clinical trials have been unsuccessful [18,19].

In this work, it was investigated whether SIS could function better for oesophageal tissue engineering if it was produced in an intact tubular form, as opposed to the regular sheet form. It was hypothesized that the lack of a seam would be an advantage not only for the potential for improved performance, but also with a view to allowing further modification of the SIS. The first stage of this was to investigate the creation of a tubular SIS. Peracetic acid under agitation has been the standard decellularization protocol for production of SIS sheets for a number of years [20,21]. However, with the SIS in tubular form, an alternative decellularization protocol was considered necessary to allow for the tissue to be adequately decellularized. Perfusion decellularization protocols have been successfully applied to a variety of tissues, and a large number of protocols and agents exist [22,23]. In this study, the two protocols selected have been used to decellularize a variety of tissues, and these two were compared to peracetic acid under agitation, along with an undecellularized control, to obtain an optimal decellularization protocol for tubular SIS. In addition to this, to draw a fair comparison between the effectiveness of the reagents in the different protocols, peracetic acid was also tested using the perfusion arrangement.

The first method was a perfusion method applied by Ott et al. [24] to decellularize intact rat hearts. This method involved the use of two detergents: sodium dodecyl sulfate (SDS), an anionic detergent, and Triton X-100 (t-octylphenoxypolyethoxyethanol), a non-ionic detergent considered to be non-denaturing [22]. Both detergents are commonly used for cell lysis applications. SDS has been used for a number of years and on a variety of tissue types, including less commonly decellularized tissues, such as the kidney and temporomandibular joint [23]. The use of Triton X-100 has also been quite prominent in the field of tissue engineering and was used for decellularization by Cortijo et al. as early as 1987 [25], when it was applied to a number of different tissues, including the ileum, arteries and muscle tissue. The method used by Ott et al. [26] was replicated by Akhyari et al. and was shown to be one of two better performing methods for whole heart decellularization in a comparison of four different protocols.

The second protocol involved a combination of sodium deoxycholate (SD) and deoxyribonuclease I (DNase). Early work done by Meezan et al. [27] isolated basement membranes from a variety of tissues, including bovine retinal and brain blood vessels, rabbit renal tubules and rat renal glomeruli, all using 4% SD and DNase. A modified version of this method was used in the decellularization of the trachea by Conconi et al. [28]. The method was used in the form of repeated cycles, which had the effect of producing a decellularized donor trachea, which was subsequently implanted into a patient [29]. This method was also then used by Totonelli et al. [30], who applied it to the decellularization of the rat small intestine using a perfusion-based method. In summary, the method described has shown a degree of effectiveness on a number of tissues when used in a perfusion-based protocol. It has been applied to scaffolds which have then gone on to be successfully implanted into a patient, and is therefore highlighted as an effective method for perfusion decellularization.

For any ECM to function *in vivo* it must be adequately decellularized, as the presence of cell membrane epitopes and xenogeneic or allogeneic DNA could result in an adverse immune response upon implantation [31]. In reviewing decellularization, Crapo and Gilbert [23] proposed three criteria for satisfactory decellularization, two of which are suitable for this work, namely: <50 ng of double stranded DNA (dsDNA) per mg of ECM (dry weight) and a lack of visible nuclear material in tissue sections stained with 4′,6-diamidino-2-phenylindole or haematoxylin and eosin (H&E). The third criterion suggested was a < 200 bp DNA fragment length, but this is beyond the scope of this work. It should be stated that these criteria are being used herein as no substantial work has been carried out which establishes the threshold level of cellular remnants in ECM materials that elicits a negative remodelling response. Additionally, should any of the protocols produce a SIS which is mechanically unsound, it would not be considered a suitable protocol.

2. Materials and methods

Frozen samples of porcine small intestine were obtained at a local abattoir from animals that were 6 months in age. The jejunum/ileum samples were cut into lengths of 20 cm and the excess mesentery tissue removed (Fig. 1a). The samples were rinsed thoroughly with deionized water to remove debris.

The SIS was isolated using slight modifications to the well-established method [32,33]. The sections of small intestine were inverted and then gently abraded using moist surgical gauze to remove the inner mucosal layer. The tissue was thoroughly washed with deionized water and then re-inverted, and the serosal layer was then taken off by first creating an incision with a scalpel, then manually removing the layer. Finally, the outer surface was carefully abraded using damp gauze to remove any remnants of the smooth muscle layers. The SIS was then carefully washed twice in deionized water for 5 min, before being stored in phosphate-buffered saline (PBS: 0.01 M phosphate buffer, 0.0027 M potassium chloride and 0.137 M sodium chloride, pH 7.4, at 25 °C). Representative tissue samples were collected throughout the process and used as control samples.

2.1. Decellularization

2.1.1. Method 1 (perfusion/immersion)

Prepared SIS samples were placed in individual glass containers, secured to adaptors and connected to a multi-channelled peristaltic pump (Watson-Marlow, Cornwall, UK). The complete arrangement is illustrated in Fig. 2. The input channels were also secured in the same containers. The solutions described below were then placed in the containers to create an isolated chamber and the pump was run to begin perfusion.

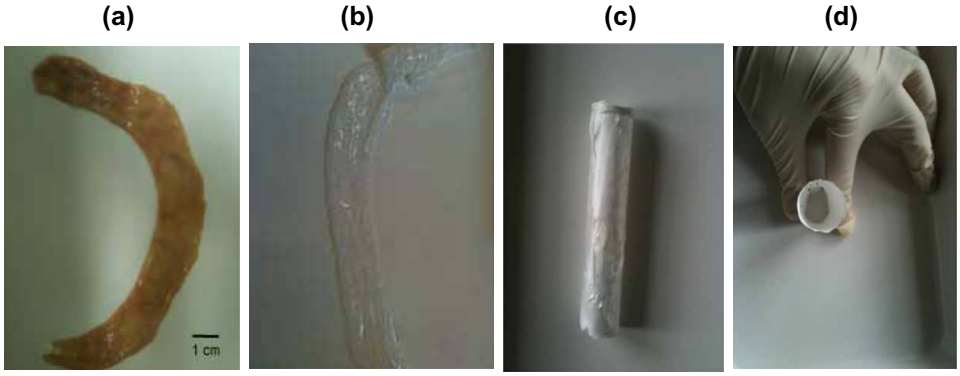

Fig. 1. (a) Porcine small intestine section prior to debridement. (b) SIS following decellularization. (c, d) Final processed form of SIS.

This approach allowed the solution to perfuse through the tissue and collect in the vessel, where it further immersed the samples while also recycling back to the pump. The benefit of this arrangement is that there is also an element of immersion decellularization which occurs on the outer surface of the SIS samples. Twelve samples were produced simultaneously using this arrangement.

2.1.1.1. Sodium dodecyl sulfate & Triton X-100 (SDS/TX). The previously described protocol was altered for this particular application in terms of reducing the number the cycles to a single cycle. Each container was filled with 350 ml of 1% solution of SDS (Sigma–Aldrich Company Ltd., Dorset, UK), then the pump was run at 500 ml h^{-1} for 12 h at room temperature (RT). The SIS was removed and thoroughly rinsed with deionized water, followed by a perfusion wash for 15 min with deionized water. The samples were then perfused with 350 ml of 1 vol.% of Triton X-100 for 30 min, rinsed and then perfused with deionized water for 15 min. The decellularized SIS was then rinsed with deionized water and soaked for 30 min in deionized water prior to being given a final rinse. All decellularized SIS was stored at 4 °C in PBS. Changes from the protocol as outlined by Akhari et al. [26] include removing steps which were suited to heart decellularization, including the use of a final stage where the perfusion is allowed to carry on for an additional 124 h in PBS containing penicillin-G, streptomycin and amphotericin B.

2.1.1.2. Sodium deoxycholate & DNase (SD/DN). The procedure here was carried out as described above. Each container was filled with 350 ml of 4% SD (Sigma–Aldrich), then the pump was run at 500 ml h^{-1} for 12 h at RT. The samples were removed and thoroughly rinsed with deionized water followed by a perfusion wash for 15 min, also with deionized water.

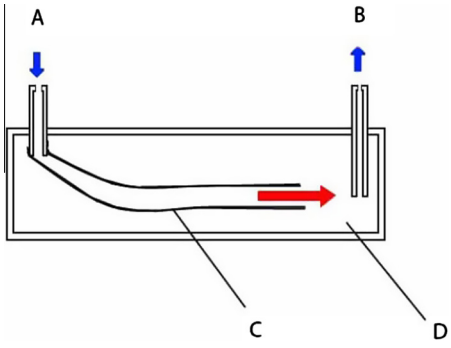

Fig. 2. Decellularization container arrangement. (a) Output from the peristaltic pump, which is connected to the SIS. (b) Return to the peristaltic pump, which is not connected to the SIS and draws the medium from the container. (c) The SIS to be decellularized. (d) Container into which the decellularization medium will collect and immerse the external surface of the SIS. The red arrow indicates the direction of flow of the perfusion decellularization medium.

The SIS was then perfused with DNase I (Sigma–Aldrich) at a quantity of 2000 kU in 300 ml of 1 M NaCl solution at RT for 3 h. At the 3 h mark an additional 1000 kU in 50 ml of 1 M NaCl was added and run for a further 1 h. This was followed by rinsing, a final perfusion and soaking in deionized water, as described previously. The samples were stored at 4 °C in PBS. The original protocol was run in a number of "cycles", and as a result the time was extended from 4–6 h to 12 h to simulate approximately two cycles. The DNase I amount was increased to 3000 kU (from 2000 kU in the original protocol), and the time was extended to 4 h (from 3 h) [34]. The additional quantity of enzyme (1000 kU) was only added in the final hour.

2.1.1.3. Peracetic acid (PAA-12h). Peracetic acid was used for the final perfusion protocol. This was run as described above but using 350 ml of a 0.1 vol.% solution of peracetic acid per length of SIS for 12 h at RT.

2.1.2. Method 2 (immersion/agitation)

2.1.2.1. Peracetic acid (PAA-2hA). SIS samples used were placed in screw-top specimen containers (150 ml capacity) and were placed on an orbital shaker (Stuart Model SSM1, Keison Products, Chelmsford, UK) to provide mechanical agitation. The containers were filled to capacity with a 0.1 vol.% solution of peracetic acid (Sigma–Aldrich), with care taken to immerse the samples completely and remove any trapped air bubbles. Decellularization in peracetic acid was carried out for 2 h under mechanical agitation at 100 rpm. The SIS samples were removed and thoroughly washed in deionized water as described previously, and stored at 4 °C in PBS. A summary of these methods are shown in Table 1.

2.2. Post-decellularization processing

The SIS sections were stretched over 1.9 cm diameter (3/4 inch) porous polyethylene tubing (60 micron pores) (Porex Corporation, Fairburn, United States). These samples were vacuum-dried in sealed sterile specimen bags and placed under low vacuum conditions (approximately 10 mbar) for 12 h to compress and dry the samples. The dried SIS samples were subsequently lyophilized by immersing in liquid nitrogen for 1 min and then placed into a vacuum freeze-drier (Heto Drywinner, Birkerod, Denmark) for 12 h. The final appearance of the processed SIS is shown in Fig. 2(c) and (d). The further processing allowed creation of SIS with a smooth and regular surface. The lyophilization also aided in extending the storage capacity of the SIS.

Table 1
Experimental conditions for SIS production.

Decellularization method	Reagents	Method	Samples tested	Processed and tested	Total number of sample sets
uSIS	Untreated	–	Untreated	Yes	2
PAA-2hA	Peracetic acid	Immersion/Agitation	2 h	Yes	2
PAA-12h	Peracetic acid	Perfusion	12 h	Yes	2
SD/DN	Sodium deoxycholate & DNase	Perfusion	4 h, 8 h, 12 h and final stage (16 h)	Yes	5
SDS/TX	Sodium dodecyl sulfate & Triton X-100	Perfusion	4 h, 8 h, 12 h and final stage (12.5 h)	Yes	5

2.3. Analysis

For the two detergent-based protocols (SDS/TX and SD/DN), sections were taken from the SIS at time points of 4, 8 and 12 h, and upon completion of the protocol, by cutting 2.5 cm segments during decellularization. Due to the presence of two stages in these protocols, i.e. a 12 h stage followed by a shorter stage, the decision was taken to test the tissue at regular intervals to assess the impact of time and the final stages.

Sections were also taken from SIS produced from the PAA-12h and PAA-2hA groups, and the untreated control SIS (uSIS). Test sections were also taken from all SIS samples following processing. The sample segments were then sectioned further and stored according to the method of analysis.

2.3.1. Histology

SIS samples to be processed for histology were fixed in 10% formalin. The samples were embedded in paraffin wax, sectioned to 3 μm thickness and stained by H&E and elastic-Van Gieson stain (EVG). Images of the sections were acquired using a light microscope (Olympus BX50, Olympus Optical Co (UK) LTD, London, UK) and analysed using Image-Pro Plus (Media Cybernetics, Rockville, USA) and Image J.

2.3.2. Scanning electron microscopy (SEM)

Non-lyophilized samples were fixed in 3% (w/v) glutaraldehyde/0.1 M CAB (sodium cacodylate) buffer for 3 h. After rinsing with PBS, the samples were dehydrated by separate 15 min immersions in graded ethyl alcohol concentrations (50, 70, 90 then 100 vol.% in deionized water), then briefly immersed in hexamethyldisilazane for critical point drying. Sections of dehydrated SIS were cut (1 mm thickness) and mounted on aluminium stubs. Lyophilized samples were cut into 0.5 mm-sided squares and directly mounted on aluminium stubs using adhesive tabs. The stubs were then placed in a desiccator cabinet for at least 12 h to ensure any acquired moisture was sufficiently removed. All sections were then sputter coated with gold/palladium (Polaron E5000, Quorum Technology, UK). The samples were then analysed using a scanning electron microscope (JEOL 5410LV SEM, JEOL UK, Herts, UK).

2.3.3. DNA quantification

To dry the non-lyophilized samples, these were first frozen and stored at −20 °C and then placed in a freeze dryer for 6 h. DNA extraction was carried out using a DNeasy Blood & Tissue Kit 50 (Qiagen, Hilden, Germany). The DNA was quantified using a Quant-iT™ DNA Assay Kit or Qubit® dsDNA HS Assay Kit (Invitrogen, Carlsbad, USA), a fluorescence plate reader (Fluoroskan Ascent, Thermo Scientific, USA) or a Qubit® Fluorometer (Invitrogen, USA).

2.3.4. Mechanical testing

Uniaxial tensile testing was carried out using a dynamic mechanical analyser (DMA 7e, Perkin-Elmer Instruments, USA). Test sections were cut into rectangular shapes of dimensions 8–14 mm in length and 5–8 mm in width, and in both the longitudinal and circumferential directions (relative to the axis of the small intestine). The ends of the samples were enclosed in wire gauze to provide grip and stability, and the samples were then clamped into the machine. The dimensions of the samples were entered into the software (Pyris, Perkin-Elmer Instruments, Akron, USA) and the distance between the two clamps was taken as the length. The tensile test was run with an increasing force value of 500 mN min^{-1}. From the stress–strain graph produced, the elastic modulus was calculated as the gradient of the elastic region of the curve (λ = stress/strain). Processed SIS was rehydrated with deionized water for 30 min, prior to testing. Samples which slipped or failed near to the clamps were ignored.

2.3.5. Statistical analysis

Basic statistical assessment of the data showed that it did not fit standard normal distribution models and therefore non-parametric statistical analysis methods were chosen. The median was deemed to be a better measure of the central tendency than the mean for this particular data, so is used in all the analyses. The group sample data was compared for significant differences using Kruskal–Wallis non-parametric analysis, which indicates the presence of significant statistical differences between individual groups. Further analysis was also carried out by post-hoc pairwise analysis (Dunnett's test). All statistical significance tests were performed using SPSS version 21 (IBM Corporation, Armonk, NY, USA).

2.3.6. Cell culture

Primary human esophageal smooth muscle cells (HESMC; ScienCell Research Laboratories, Carlsbad, CA, USA) were cultured in Dulbecco's modified Eagle's medium (Gibco, Life Technologies, Paisley, UK) supplemented with 10% foetal bovine serum (Gibco) and 1% penicillin–streptomycin (Gibco) at 37 °C in air, with 5% CO_2 and 95% relative humidity. Cells from passages 3–6 were used for experiments.

2.3.7. Biocompatibility assay

A CellTiter 96 AQueous Non-Radioactive Cell Proliferation Assay (Promega, Southampton, UK) was used to assess the enzymatic activity of HESMC as an indication of biocompatibility, in accordance with ISO 10993 parts 5 [35] and 12 [36] and the manufacturer's protocol. Briefly, HEMSC were seeded at a density of 100,000 cells cm^{-2} on PAA-12h, PAA-2hA, SDS/TX, SD/DNA, uSIS and a commercial scaffold, with tissue culture plastic (TCP) as a control. The commercial scaffold was Biodesign® (Cook Medical, Bloomington, USA) and was used in this instance only to provide a potential alternative to TCP as a control. Cell culture inserts (CellCrown, Scaffdex Ltd., Tampere, Finland) were used to pull the samples taut and suspend them within the 24-well plates with the cells seeded on the abluminal surface, with the exception of the commercial scaffold, which did not have a specified orientation. The scaffolds were all hydrated with 200 μl of medium approximately 30 min prior to seeding cell. After incubation for 24 or 96 h, medium was aspirated from the cells and replaced with one part of MTS solution in six parts of medium, which consists of (3-(4,5-dimethylthiazol-2-yl)-5-(3-carboxymethoxyphenyl)-2-(4-sulfophenyl)-2H-tetrazolium) (MTS dye) and the electron

coupling agent phenazine methosulfate. MTS is metabolized to form formazan in the mitochondria of living cells, resulting in a colour change from yellow to brown that is indicative of cell number. After sufficient colour change was observed (after incubation for 1–1.5 h), absorbance was measured at 490 nm, with a reference wavelength of 630 nm. The metabolic activity of cells residing on each scaffold was normalized to the TCP control, specific to each time point. Between time points, the MTS-containing medium was aspirated, the cells were rinsed with PBS, and the medium was replaced with fresh cell culture medium.

3. Results

3.1. Histology

Staining with H&E revealed the presence of visible and distinct nuclei in all samples (Fig. 3), with the number of nuclei in the final samples being SDS/TX < PAA-12h < SD/DN < PAA-2hA < uSIS (Fig. 6a). The numbers of visible nuclei per square micrometre were found to be far higher in the uSIS control and PAA-2hA groups than in the final stages of SDS/TX, SD/DN and PAA-12h. The SDS/TX group was observed to have the lowest number of histologically visible nuclei per square micrometre of visible tissue by a substantial margin. Staining with EVG showed a quite even dispersal of black-stained elastin fibres throughout the intestinal tissue. The decellularization process did not appear to result in any visible loss of elastin fibres by any of the protocols (Fig. 4).

3.2. SEM

The use of SEM imaging did not reveal any visible differences between samples of the five groups (Fig. 5). There were also no visible differences between samples taken from different time points during the longer multi-stage protocols (SDS/TX and SD/DN). The fibrous structure of the pre-processed SIS samples was clearly visible on some images (Fig. 5d). The processed form of the SIS produced a characteristic sheet-like regular appearance (Fig. 5h) in most samples, with the exception of the processed PAA-12h, which had a characteristic appearance of a more cracked surface with defects (Fig. 5f and g).

3.3. DNA quantification

DNA quantification revealed that the SDS/TX group produced samples with the lowest levels of DNA following the decellularization process (Fig. 6b). SD/DN also proved to be effective at decellularization producing DNA levels well below the uSIS control. The level of DNA present in the PAA-2hA group was not significantly different to that of the control. The level of DNA present in the PAA-12h group was not significantly different from the control but was significantly lower that the PAA-2hA group.

It was also observed that SD/DN produced no appreciable difference in the DNA quantity detected between the 12 h time point and the final stage (16 h), indicating that the introduction of the enzyme DNase did not affect the quantity of the DNA remaining in the SIS.

3.4. Mechanical analysis

In longitudinal testing, the elastic modulus values did not vary significantly between the specimens with the exception of the PAA-12h, which had increased values in both directions, with the longitudinal value being exceptionally high when compared to the other groups (Fig. 7a). It was observed that, following decellularization, the SIS produced from the PAA-12h protocol was physically different to all other SIS samples when handled. The SIS in this group took on a more ridged and less pliable texture not observed in any of the other groups. Lyophilization of the samples did not affect the elastic modulus values, with the exception of the PAA-12h group, which fell dramatically, and the SDS/TX group, which, when compared longitudinally with the pre-lyophilized form, showed a significant increase.

The yield stress was considered a useful parameter as the data mirrored that of the failure and indicates the stress at which the tissue undergoes mechanical compromise. The calculated yield stress values showed no significant change between the specimens with the exception of the PAA-12h sample, which again was found to be significantly larger, particularly in the longitudinal direction but also circumferentially, when compared to the other pre-lyophilized SIS (Fig. 7b). The lyophilization here was found to cause slight increases in all samples, with the increase in SDS/TX being quite substantial, though with the exception of the PAA-12h group, which fell in longitudinal testing. The only significant circumferential increase was found in the PAA-12h specimens, which showed a substantial increase in the yield strain value. Again, it should be noted here that the PAA-12h SIS produced greatly different behaviour when compared to the other samples.

The failure strain was calculated as the actual point of failure of the testing sample during the tensile test. In the longitudinal testing,

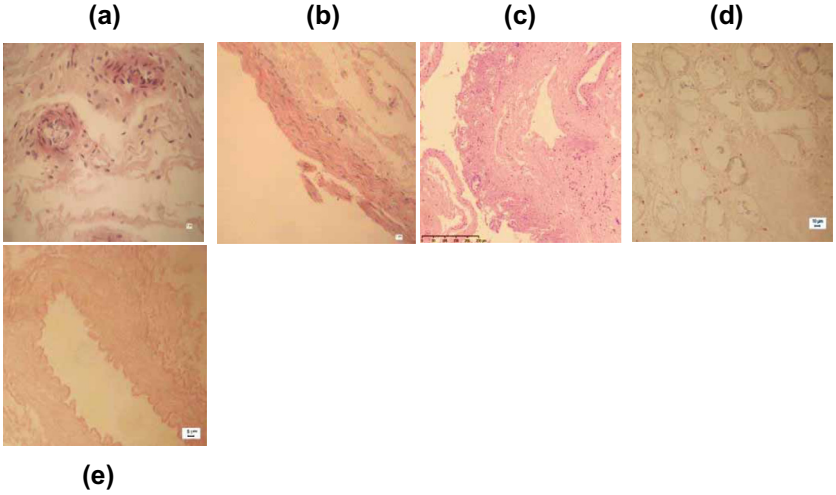

Fig. 3. Histological images (stained with H&E): (a) uSIS, (b) PAA-2hA, (c) PAA-12h, (d) SD/DN and (e) SDS/TX.

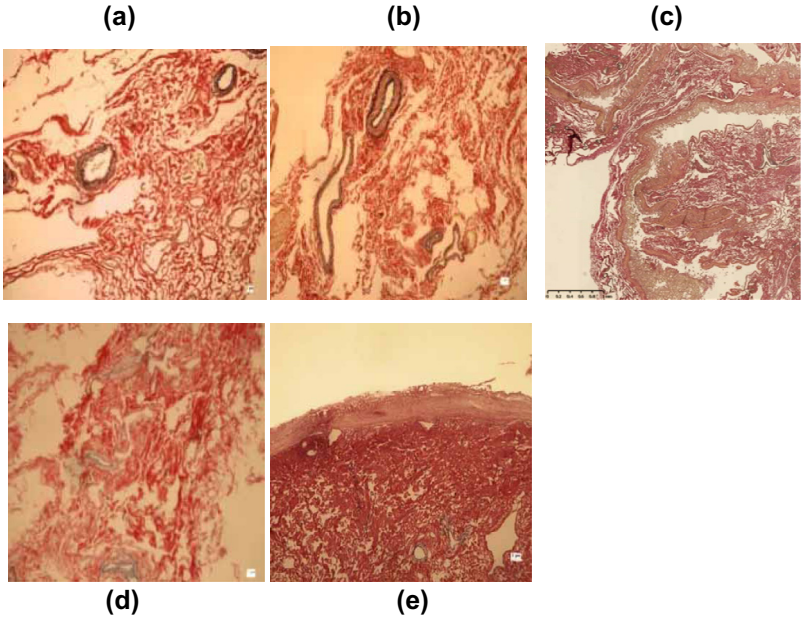

Fig. 4. Histological images of decellularizing SIS and the controls (stained with EVG): (a) uSIS, (b) PAA-2hA, (c) PAA-12h, (d) SD/DN and (e) SDS/TX.

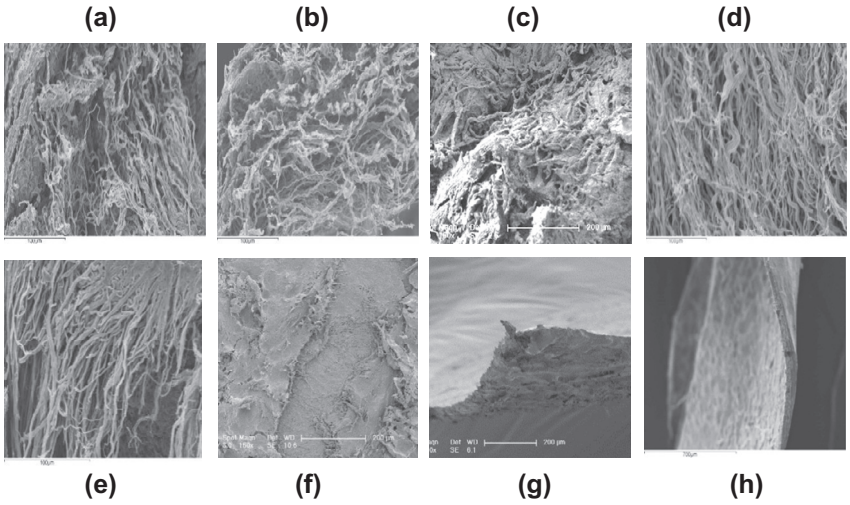

Fig. 5. SEM images of SIS from the protocol groups. All are taken from a cross-sectional view unless specified: (a) uSIS, (b) PAA-2hA, (c) PAA-12h, (d) SD/DNase, (e) SDS/TX, (f) luminal view of processed PAA-12h, (g) processed PAA-12h and (h) processed SD/DNase.

the values for the specimens from the SDS/TX, SD/DN and PAA-12h groups were all found to be similar to the control uSIS or the PAA-2hA group (Fig. 7c). It was also noted that the value for PAA-12h was found to be very low (39.29%), with a very low error, indicating that, while the PAA-12h was very stiff and gave high yield strength values, the material had a greatly reduced elasticity when compared to the control uSIS or the other samples. In circumferential testing, only the PAA-12h failure strain value was found to be significantly lower than that of the control uSIS. Following lyophilization, the PAA-12h SIS was observed to change in failure strain behaviour, with the value increasing following the processing.

The results from the 12 h detergent decellularization stages (at time points of 4, 8 and 12 h) in both the SD/TX and SD/DN groups (Fig. 8) do not appear to indicate any quantifiable time-dependant changes in the mechanical properties of the SIS by the criteria which were investigated.

3.5. Biocompatibility

The results of the biocompatibility assay were expressed in terms of metabolic activity and are represented as a percentage in relation to the TCP control for that time point (Fig. 9). At day 1 (24 h), the SIS specimens from the PAA-2hA and PAA-12h groups were found to have metabolic activity levels which were similar to the TCP control, while the SD/DN and the commercial SIS groups were found to be elevated at to levels 1.5 and 2 times greater, respectively. The uSIS group was found to have highly elevated metabolic activity, with the average value being approximately 4 times that of the control group TCP group, indicating a very rapid increase in the metabolic activity of the cells. Conversely, the SDS/TX group was found to have significantly lower values than the control TCP and all other samples, indicating lower biocompatibility.

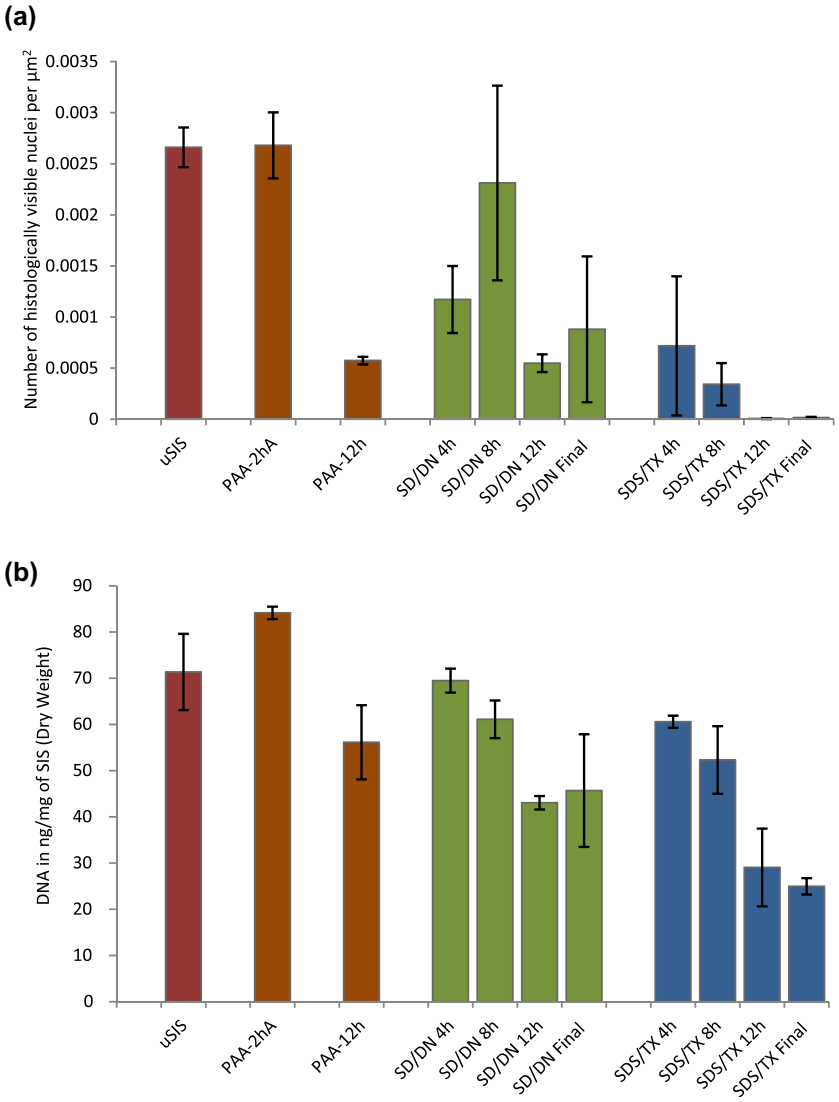

Fig. 6. (a) The average number of distinct nuclei counted per square micrometre of SIS for all SIS groups. Analysis was carried out on images taken of H&E-stained histological sections, with random sites chosen and the nuclei counted using software (Image J) (n = 10–20). All counts were then averaged together for each stage. Error bars show the standard error. (b) DNA quantification values (ng per mg dry weight) for the three protocols and the control, with each column representing the concentration of DNA at various time points in the decellularizing protocols, including the processed SIS (n = 4). Error bars show the standard error.

At day 4 (96 h), all specimens showed an increase in metabolic activity from the levels at day 1, including the TCP group. The SDS/TX specimens still induced very low activity levels, which at day 4 remained lower than all other groups at day 1, indicating ongoing cytotoxicity. Both PAA groups performed similarly to the TCP control group, indicating a reasonable degree of biocompatibility. At day 4, the SD/DN, commercial SIS and uSIS groups all showed numbers at least twice that of the relative TCP value. While the uSIS group finished with the highest activity level, there was also a decrease relative to the control, indicating a levelling off of the sudden increase in the first 24 h.

4. Discussion

The aim of this study was to evaluate commonly used decellularization protocols to create tubular SIS which has a sufficient level of decellularization to function as a tissue engineering scaffold, yet possesses mechanical properties that are either minimally affected or, ideally, unaffected by the decellularization process. The perfusion method has not been applied to SIS previously, but was hypothesized to be suitable on account of the shape of the tubular SIS.

The data from histological evaluation and quantitative DNA analysis show that the most effective protocol was the SDS/TX. The SIS produced by this method largely achieved both the criteria highlight by Crapo and Gilbert [23]: being below the 50 ng of dsDNA per mg of ECM (dry weight) and having no histologically visible nuclei. While it is understood that no work has been carried out that evaluates these criteria as indicators of sufficient decellularization, it is logical that minimizing the amount of foreign DNA present in any type of graft tissue would likely increase the chance of successful implantation due to a reduced immune response. It was also found that both detergent-based perfusion methods produced SIS with DNA below the 50 ng of dsDNA per mg of ECM (dry weight) threshold, and that both methods using peracetic acid did not adequately decellularize SIS, though there was a significant difference between the two. The question arises as to whether this is due to the effectiveness of the reagents or the time duration of the protocols, or is a result of the physical process of the protocols themselves.

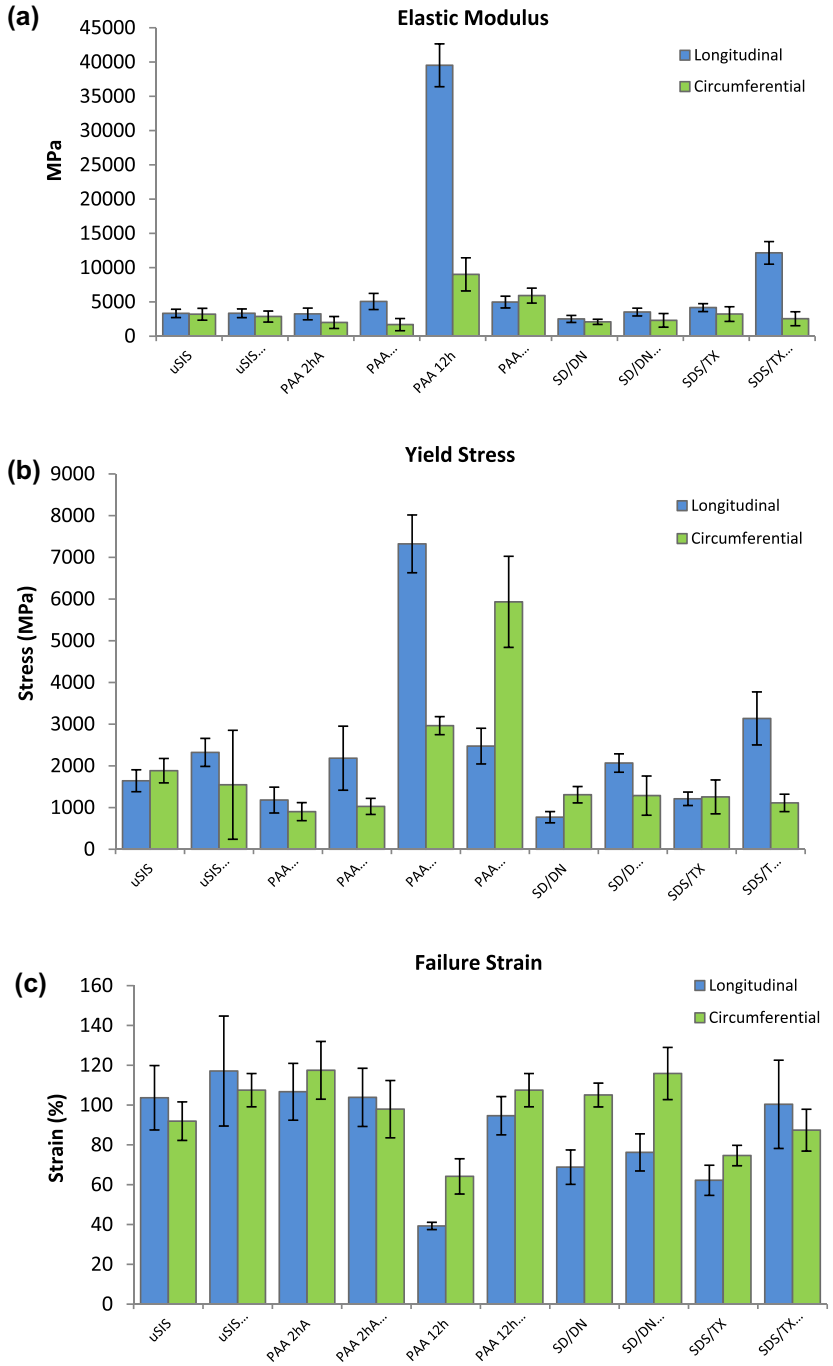

Fig. 7. Mechanical tensile testing data from all final stage SIS groups, along with the lyophilized forms (n = 12). (a) Elastic modulus values (MPa). (b) Yield stress values (MPa). (c) Failure strain (%). Error bars show the standard error.

When the effectiveness of the reagents is considered, there is evidence to suggest that, using a number of different criteria, they can all be considered highly effective at decellularization. When applied to sheet SIS, peracetic acid is known to be an effective reagent for decellularization. SDS and Triton X-100 have also been shown, by Oliveira et al. [37], to have the capacity to decellularize SIS individually to levels below 50 ng of dsDNA per mg using concentrations as low as 0.1% over a 24 h period under agitation. SD, while not having been used on SIS, has been shown to decellularize the small intestine in a rat model [30]. Consequently, all three agents are likely to be effective at decellularizing SIS. Therefore, the failure of the SIS to decellularize in this study particularly using PAA is likely not to be due entirely to the effectiveness of the reagent but is more likely to be due to the decellularization methods or the shape and structure of the tissue.

The length of time the protocols are run is another important factor. The level of DNA present in the detergent-based protocols (Fig. 6b) can be seen to steadily decrease over time, which undoubtedly shows that time is a vital component of the decellularization process. Time has also been shown to effect peracetic acid decellularization, and halving the decellularization time to 1 h results in elevated levels of DNA when compared samples run for 2 h [12]. In addition to this, the increased effectiveness of the PAA-12h perfusion protocol (in comparison to the PAA-2hA

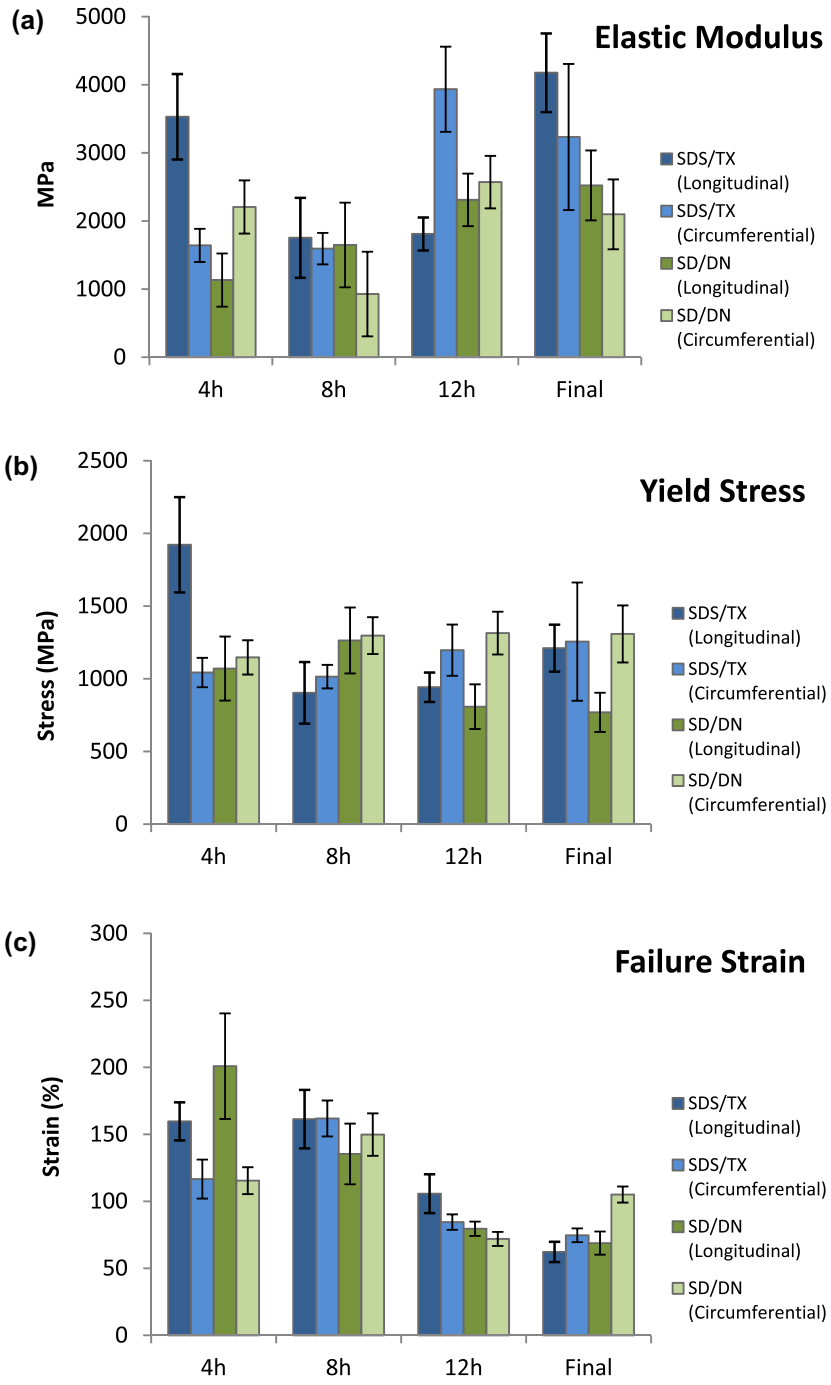

Fig. 8. Mechanical data from tensile testing SIS from the two detergent-based protocols (SDS/TX and SD/DN) taken from different time points during the decellularization process. The three criteria used in the analysis are: (a) elastic modulus (MPa), (b) yield stress (MPa) and (c) failure strain (%). Error bars show the standard error.

group) indicates that time likely improves the effectiveness of peracetic acid decellularization; however, while the amount of DNA was reduced slightly, the number of nuclei visible suggests a less than optimum level of decellularization (Fig. 3c).

The final difference between the protocols was the decellularization arrangements themselves. As mentioned above, there are no examples of SIS being decellularized using a perfusion arrangement and no work where the intact tubular size was consistently studied. Perfusion decellularization has been used on rat small intestine using 4% SD/DNase, and this was found to be an effective means of decellularization; however, the analysis was limited to the histological means [38]. Multi-organ decellularization of rat tissues using SDS perfusion has also been shown to be effective at decellularization [39]. In the case of this work, however, it is unclear whether the SIS was actually undergoing true perfusion through the SIS itself. SIS is a largely impermeable tissue and, given the low flow rates used, it is highly unlikely that the decellularization agents perfused through the thickness of the tissue. The combination of a constant flow of decellularizing agents over the luminal surface of the SIS in addition to the circulating agents on the outer surface, however, has likely produced an environment where suitable decellularization can occur simultaneously on both surfaces and consequently provides a working method for decellularizing tubular SIS.

One of the major observations in the mechanical testing was the extreme variations in the data produced by the PAA-12h

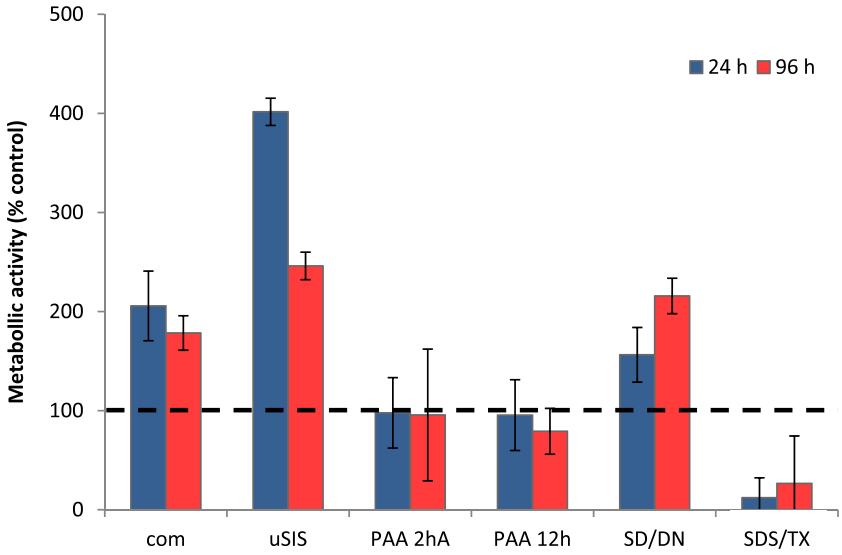

Fig. 9. Metabolic activity of the cells (HESMC) cultured on the scaffold groups. The metabolic activity was normalized in relation to the control (TCP with the same surface area), and is expressed here as a percentage of the control, specific to each time point. The dashed line indicates the metabolic activity of the TCP control at each time point.

protocol. The large increases in the elastic modulus and the yield stress values were also accompanied by a drastic drop in the failure strain to the lowest of all the SIS samples, at just below 40%. This is indicative of SIS tissue which has lost a high degree of elasticity when compared to the control; as a result, this SIS can be reasonably excluded from consideration. Furthermore, the human oesophagus also extended by up to 50% under normal conditions, and any material which has a failure strain below this level risks failing and compromising the integrity of the construct [40,41]. The SIS produced by peracetic acid under agitation (PAA-2hA) appeared to match the control and the SIS from the detergent-based protocols in its mechanical behaviour; however, as already described, it was poorly decellularized and is therefore not suitable as a scaffold. The short exposure of the SIS to the peracetic acid is the likely cause of the difference between the two protocols. Currently there does not appear to be any definitive consensus on the effects of individual decellularization agents on the mechanical properties of many of the commonly used decellularized tissues [23]. It has been shown that some acids, when used on ECM, can alter its mechanical properties. An example of this is acetic acid, which has been shown to alter the stress–strain behaviour of bovine pericardium [38]. Peracetic acid has not been reported to alter the mechanical properties of SIS, though, as in the case here, the time of exposure was commonly limited to 2 h [22,39].

The two detergent-based protocols also produced decellularized SIS, which was not adversely affected by the decellularization process according to the three criteria which were used for evaluation. Of the two protocols, only SDS/TX produced SIS with high values for all three criteria, particularly in terms of the lyophilized form. It should be mentioned that detergents have also been known to disrupt the ECM matrix; however, this was not observed in this study [23]. A possible reason for this is that both of these protocols were adapted in this study to reflect the nature of the SIS, which only consists of a thin layer of predominantly ECM, and were therefore run for a shorter time. In the case of other tissues, these profusion protocols are run for a large number of repeated cycles. A variation of the SD/DNase protocol has been used to decellularize a human donor trachea, a process that takes multiple cycles, though it was found that, between cycles 18 and 22, the mechanical properties were so negatively impacted as to render the trachea ineffective [34]. Consequently, the limited exposure of the detergents to the tissue in this work could be the reason for the preservation of the mechanical properties.

A number of inconsistencies were observed in the mechanical testing between the longitudinal and circumferential tensile data. This was attributed to the native anisotropy found to be present in SIS having a high degree of complexity [42]. If both axes are secured simultaneously and a force is applied along one axis, this would directly result in changes in the stress–strain behaviour along the other axis. This behaviour was also found to be asymmetric with the application of a set force along the longitudinal axis, resulting in changes to the circumferential stress–strain behaviour which were more pronounced than if the axes were reversed [43]. This anisotropy has been explained by the angular distribution of the fibres within the ECM of the submucosal layer [44]. These fibres have been described as two distinct populations of fibres orientated at approximately ±30° [42,43]. Sacks and Gloeckner [43] found the ±30° orientated layers to be part of local subdivisions within the tissue, which can vary along its length. This is also reinforced by the description of the fibres being aligned in a spiral, which can be considered conducive to peristalsis [45].

The vacuum-compression and lyophilization of the SIS was found to alter its mechanical properties. The exact mechanism for these changes is not entirely clear, though the differences between the longitudinal and circumferential directions can be partially explained in terms of the native anisotropy of the tissue, as mentioned above. What can be observed from the data in Fig. 7 is that there were changes, at least along the longitudinal direction, particularly in terms of the failure strain for all samples. A possible mechanism for this is that the vacuum compression of the SIS results in an increased level of interaction between the ECM components – particularly the collagen fibres – present, thereby altering the mechanical properties. It should be noted that, following rehydration, the processed samples did not expand to the same thickness as the pre-processed SIS samples. In addition to changes in the mechanical properties, it has been shown that processing decellularized SIS can cause a change to the *in vivo* properties. When vacuum-pressed SIS was compared to lyophilized SIS, the vacuum-pressed SIS was found to be more resistant to enzymatic degradation, and angiogenesis was also observed to occur at a slower rate due to slower rates of cell infiltration. The compressed SIS test was found to have a far lower degree of porosity and retained a compressed appearance after rehydration [46].

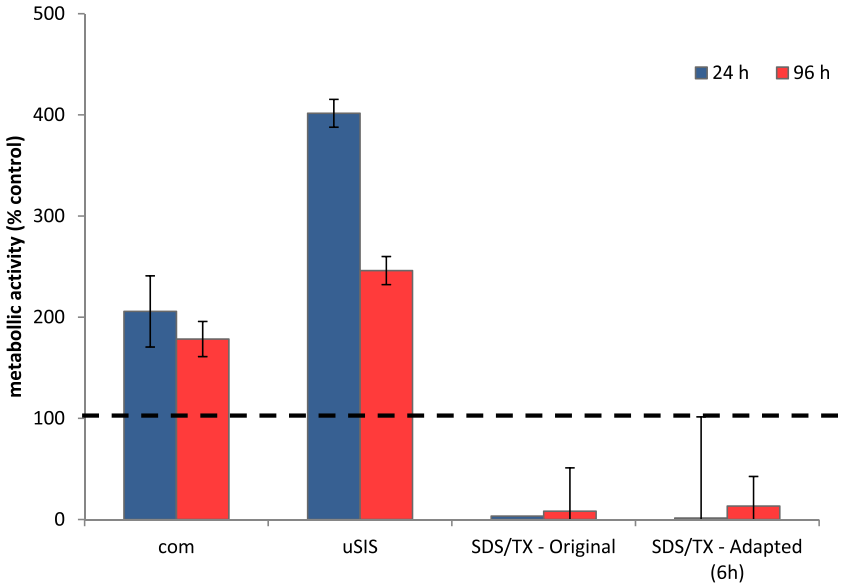

Fig. 10. Metabolic activity of the cells (HESMC) cultured on the SDS/TX scaffolds, showing the difference between the SDS/TX original protocol and an adapted protocol with an extended washing regime (increased to 6 h, with a continuous flow of fresh deionized water). The metabolic activity was normalized in relation to the control (TCP with the same surface area), and is expressed here as a percentage of the control, specific to each time point. The commercial scaffold was added as a reference point for biocompatibility. The dashed line indicates the metabolic activity of the TCP control at each time point.

The biocompatibility of the scaffolds is an important consideration for their potential future use. The data here showed clear differences between decellularization protocols. While both peracetic acid protocols showed a good degree of biocompatibility, cells cultured on the SDS/TX had lower levels of metabolic activity than all the other samples, including the control. While the SIS produced from this method was found to be most ideal both mechanically and in terms of the decellularization, this level of biocompatibility makes it highly unsuitable. Furthermore, follow-up work (Fig. 10), where SDS/TX was created and then washed for 6 h using an improved washing method, failed to significantly improve the biocompatibility. This protocol involves the use of two separate detergents which have each been shown to be cytotoxic, i.e. SDS and Triton X-100, and with this increased exposure there is also an increased likelihood of some detergent being retained within the SIS itself.

SD is also a cytotoxic detergent and it should be noted that, in the SD/DN protocol, which had the best biocompatibility of all the decellularized SIS produced, the SIS was exposed to a 4 h rinse with a salt solution (containing the DNase) following detergent exposure. This could potentially have aided in removing the detergent sufficiently from the SIS to produce the observed results. It should be noted that, while SIS produced with the SD/DN protocol had a very high biocompatibility (higher than the commercial SIS), the presence of the DNase enzyme, though likely to have a minimal effect on cell growth in vitro, may have a more negative effect if applied *in vivo*.

The uSIS demonstrated a high degree of biocompatibility, which could be explained if the internal structure was preserved and the tissue components retained. An intact ECM, in addition to any remaining growth factors, could potentially stimulate cellular activity. While testing of this scaffold indicated acceptable biocompatibility *in vitro*, it would nevertheless be unsuitable for *in vivo* applications due to a potential immune response.

5. Conclusion

In conclusion, the conventional peracetic acid/agitation method for SIS decellularization is not suitable for SIS when made in intact tubular form. The primary reason for this is the insufficient level of decellularization. Peracetic acid, when used over 12 h with the perfusion method, was also found to be unsuitable, owing to a drastic drop in the elasticity of the tissue following decellularization. The two detergent/perfusion protocols were found not only to provide adequate decellularization of the SIS, but in several instances were found to possess less adversely affected mechanical properties over the SIS produced from peracetic acid or the control particularly following processing. There are, however, limitations associated with both methods. It was concluded that SDS/TX was the most suitable protocol for producing scaffolds because: it caused the highest level of decellularization therefore posed the least risk of an immune response and/or graft rejection; it produced the SIS with the most advantageous properties following the processing stage; and finally, the protocol lacked enzymes as used in SD/DNase, which may potentially increase the risk of rejection. However, as shown in Fig. 10, the biocompatibility of the scaffold cannot be improved even by increasing the washing time to 6 h and using an improved washing method. Consequently, whilst there may be some merit in research into improving the wash cycle, it was deemed that longer time periods would not be practical. It was observed that, whilst SD/DN may show acceptable *in vitro* biocompatibility and suitable mechanical properties, it has the limitation of using the DNase enzyme, which may be unsuitable for clinical application. In conclusion, SIS produced using SD with a stage to eliminate the DNase enzyme could potentially be the ideal basis for future work.

Acknowledgement

This work was supported by the Priority Research Centers Program (No. 2009-0093829) through the National Research Foundation, Republic of Korea.

Appendix A. Figures with essential colour discrimination

Certain figures in this article, particularly Figures 1–4 and 6–10, are difficult to interpret in black and white. The full colour images

can be found in the on-line version, at http://dx.doi.org/10.1016/j.actbio.2014.08.024.

References

[1] Holland AJA, Fitzgerald DA. Oesophageal atresia and tracheo-oesophageal fistula: current management strategies and complications. Paediatr Respir Rev 2010;11:100–7.
[2] Hartel M, Wente. Surgical treatment of oesophageal cancer. Dig Dis 2004;22:213–20.
[3] Ritchie A, Chian K, Beckstead B, Ratner B. Esophagus: a tissue engineering challenge. In: Bronzino JD, editor. Tissue engineering and artificial organs. Boca Raton, FL: CRC Press; 2006. pp. 54-1–19.
[4] Spitz L, Kiely EM, Drake DP, Pierro A. Long-gap oesophageal atresia. Pediatr Surg Int 1996;11:462–5.
[5] Totonelli G, Maghsoudlou P, Georgiades F, Garriboli M, Koshy K, Turmaine M, et al. Detergent enzymatic treatment for the development of a natural acellular matrix for oesophageal regeneration. Pediatr Surg Int 2013;29:87–95.
[6] Ludman L, Spitz L. Quality of life after gastric transposition for oesophageal atresia. J Pediatr Surg 2003;38:53–7.
[7] Abou Neel EA, Bozec L, Knowles JC, Syed O, Mudera V, Day R, et al. Collagen – emerging collagen based therapies hit the patient. Adv Drug Deliv Rev 2013;65:429–56.
[8] Valentin J, Badylak J, McCabe G, Badylak S. Extracellular matrix bioscaffolds for orthopaedic applications – a comparative histologic study. J Bone Joint Surg Am 2006;88:2673–86.
[9] VoytikHarbin SL, Brightman AO, Kraine MR, Waisner B, Badylak SF. Identification of extractable growth factors from small intestinal submucosa. J Cell Biochem 1997;67:478–91.
[10] Allman AJ, McPherson TB, Badylak SF, Merrill LC, Kallakury B, Sheehan C, et al. Xenogeneic extracellular matrix grafts elicit a Th2-restricted immune response. Transplantation 2001;71:1631–40.
[11] Bach FH, Ferran C, Hechenleitner P, Mark W, Koyamada N, Miyatake T, et al. Accommodation of vascularized xenografts: expression of "protective genes" by donor endothelial cells in a host Th2 cytokine environment. Nat Med 1997;3:196–204.
[12] Keane TJ, Londono R, Turner NJ, Badylak SF. Consequences of ineffective decellularization of biologic scaffolds on the host response. Biomaterials 2012;33:1771–81.
[13] Brown BN, Valentin JE, Stewart-Akers AM, McCabe GP, Badylak SF. Macrophage phenotype and remodeling outcomes in response to biologic scaffolds with and without a cellular component. Biomaterials 2009;30:1482–91.
[14] Badylak SF, Taylor D, Uygun K. Whole-organ tissue engineering: decellularization and recellularization of three-dimensional matrix scaffolds. In: Yarmush ML, Duncan JS, Gray ML, editors. Annual review of biomedical engineering, vol. 13. Palo Alto, CA: Annual Reviews; 2011. p. 27–53.
[15] Badylak S, Meurling S, Chen M, Spievack A, Simmons-Byrd A. Resorbable bioscaffold for esophageal repair in a dog model. J Pediatr Surg 2000;35:1097–103.
[16] Clough A, Ball J, Smith GS, Leibman S. Porcine small intestine submucosa matrix (surgisis) for esophageal perforation. Ann Thorac Surg 2011;91. e99–e100-e99-e.
[17] Doede T, Bondartschuk M, Joerck C, Schulze E, Goernig M. Unsuccessful alloplastic esophageal replacement with porcine small intestinal submucosa. Artif Organs 2009;33:328–33.
[18] Derwin KA, Baker AR, Spragg RK, Leigh DR, Iannotti JP. Commercial extracellular matrix scaffolds for rotator cuff tendon repair – biomechanical, biochemical, and cellular properties. J Bone Joint Surg Am 2006;88A:2665–72.
[19] Ricchetti ET, Aurora A, Iannotti JP, Derwin KA. Scaffold devices for rotator cuff repair. J Shoulder Elbow Surg 2012;21:251–65.
[20] Hodde JP, Record RD, Tullius RS, Badylak SF. Retention of endothelial cell adherence to porcine-derived extracellular matrix after disinfection and sterilization. Tissue Eng 2002;8:225–34.
[21] Badylak SF, Tullius R, Kokini K, Shelbourne KD, Klootwyk T, Voytik SL, et al. The use of xenogeneic small intestinal submucosa as a biomaterial for Achilles' tendon repair in a dog model. J Biomed Mater Res 1995;29:977–85.
[22] Gilbert TW, Sellaro TL, Badylak SF. Decellularization of tissues and organs. Biomaterials 2006;27:3675–83.
[23] Crapo P. Gilbert. An overview of tissue and whole organ decellularization processes. Biomaterials 2011;32:3233–43.
[24] Ott HC, Matthiesen TS, Goh S-K, Black LD, Kren SM, Netoff TI, et al. Perfusion–decellularized matrix: using nature's platform to engineer a bioartificial heart. Nat Med 2008;14:213–21.
[25] Cortijo J, Dixon JS, Foster RW, Small RC. Influence of some variables in the Triton X-100 method of skinning the plasmalemmal membrane from guinea pig trachealis muscle. J Pharmacol Methods 1987;18:253–66.
[26] Akhyari P, Aubin H, Gwanmesia P, Barth M, Hoffmann S, Huelsmann J, et al. The quest for an optimized protocol for whole-heart decellularization: a comparison of three popular and a novel decellularization technique and their diverse effects on crucial extracellular matrix qualities. Tissue Eng Part C Methods 2011;17:915–26.
[27] Meezan E, Hjelle JT, Brendel K, Carlson EC. A simple, versatile, nondisruptive method for the isolation of morphologically and chemically pure basement membranes from several tissues. Life Sci 1975;17:1721–32.
[28] Conconi MT, De Coppi P, Di Liddo R, Vigolo S, Zanon GF, Parnigotto PP, et al. Tracheal matrices, obtained by a detergent-enzymatic method, support in vitro the adhesion of chondrocytes and tracheal epithelial cells. Transpl Int 2005;18:727–34.
[29] Macchiarini P, Jungebluth P, Go T, Asnaghi MA, Rees LE, Cogan TA, et al. Clinical transplantation of a tissue-engineered airway. Lancet 2008;372:2023–30.
[30] Totonelli G, Maghsoudlou P, Garriboli M, Riegler J, Orlando G, Burns AJ, et al. A rat decellularized small bowel scaffold that preserves villus-crypt architecture for intestinal regeneration. Biomaterials 2012;33:3401–10.
[31] Gilbert TW, Freund JM, Badylak SF. Quantification of DNA in biologic scaffold materials. J Surg Res 2009;152:135–9.
[32] Lantz GC, Badylak SF, Coffey AC, Geddes LA, Blevins WE. Small intestinal submucosa as a small-diameter arterial graft in the dog. J Invest Surg 1990;3:217–27.
[33] Badylak SF. Small intestinal submucosa as a large diameter vascular graft in the dog. J Surg Res 1989;47:74–80.
[34] Jungebluth P, Go T, Asnaghi A, Bellini S, Martorell J, Calore C, et al. Structural and morphologic evaluation of a novel detergent–enzymatic tissue-engineered tracheal tubular matrix. J Thorac Cardiovasc Surg 2009;138:586–93.
[35] ISO 10993-5:2009(en) Biological evaluation of medical devices – Part 5: Tests for in vitro cytotoxicity.
[36] ISO 10993-12:2007(en) Biological evaluation of medical devices – Part 12: Sample preparation and reference materials.
[37] Oliveira AC, Garzon I, Ionescu AM, Carriel V, Cardona Jde L, Gonzalez-Andrades M, et al. Evaluation of small intestine grafts decellularization methods for corneal tissue engineering. PLoS ONE 2013;8:e66538.
[38] Maghsoudlou P, Totonelli G, Loukogeorgakis SP, Eaton S, De Coppi P. A Decellularization methodology for the production of a natural acellular intestinal matrix. J Vis Exp 2013;80:e50658.
[39] Park KM, Woo HM. Systemic decellularization for multi-organ scaffolds in rats. Transpl Proc 2012;44:1151–4.
[40] Yang W, Fung TC, Chian KS, Chong CK. Directional, regional, and layer variations of mechanical properties of esophageal tissue and its interpretation using a structure-based constitutive model. J Biomech Eng-Trans ASME 2006;128:409–18.
[41] Tan JY, Chua CK, Leong KF, Chian KS, Leong WS, Tan LP. Esophageal tissue engineering: an in-depth review on scaffold design. Biotechnol Bioeng 2012;109:1–15.
[42] Orberg J, Baer E, Hiltner A. Organization of collagen fibers in the intestine. Connect Tissue Res 1983;11:285–97.
[43] Sacks MS, Gloeckner DC. Quantification of the fiber architecture and biaxial mechanical behavior of porcine intestinal submucosa. J Biomed Mater Res 1999;46:1–10.
[44] Lanir Y. A structural theory for the homogeneous biaxial stress–strain relationships in flat collagenous tissues. J Biomech 1979;12:423–36.
[45] He M, Callanan A. Comparison of methods for whole organ decellularization in tissue engineering of bio-artificial organs. Tissue Eng Part B Rev 2012;19:19.
[46] Janis AD, Johnson CC, Ernst DM, Brightman AO. Structural characteristics of small intestinal submucosa constructs dictate in vivo incorporation and angiogenic response. J Biomater Appl 2011.